ACADEMIC PRESS

Available online at www.sciencedirect.com

SCIENCE DIRECT®

Journal of Sound and Vibration 260 (2003) 3–17

JOURNAL OF SOUND AND VIBRATION

www.elsevier.com/locate/jsvi

Statistical characteristics of pressure oscillations in a premixed combustor

Tim C. Lieuwen*

School of Aerospace Engineering, Georgia Institute of Technology, Atlanta, GA 30332-0150, USA

Received 29 January 2001; accepted 25 March 2002

Abstract

This paper describes an investigation of the statistical characteristics of self-excited and noise-driven pressure oscillations in a premixed combustor. This work was motivated by observations that certain characteristics of these oscillations appear random and cannot be entirely characterized within a deterministic framework (e.g., spontaneous, noise-induced transitions of the combustor from stable to unstable operation or cycle-to-cycle variations in the oscillating pressure). In an effort to elucidate these stochastic elements, we performed an analysis of cycle-to-cycle variations in combustor pressure whose results are described in this paper. Data obtained from our combustor shows that the probability density function of the amplitude of these oscillations transitions from a Rayleigh to a Gaussian-type distribution as the combustor moves from stable to unstable operation. These data also show that the instability phase is nearly uniformly distributed; i.e., there is no phase value with maximum probability of occurrence. We also describe a theoretical analysis of the statistical features of a non-linear combustor model that is forced by random noise. Solutions of this model are presented and shown to be in agreement with measured data. The good agreement between the predictions and measured data suggest that the analysis presented in this paper provides a useful framework for interpreting many other apparently random features of combustor stability characteristics; for example, cyclic variability, ''fuzziness'' in stability boundaries, or noise-induced transitions.

1. Introduction

This paper describes a study of the statistical features of pressure oscillations in a premixed combustor. These oscillations are driven by interactions between unsteady flow and heat release

*Tel.: +1-404-894-3041; fax: +1-404-894-3041.
E-mail address: tim.lieuwen@aerospace.gatech.edu (T.C. Lieuwen).

0022-460X/03/$ - see front matter
PII: S0022-460X(02)00895-7

processes in the combustor, and often lead to detrimental, large amplitude oscillations of the combustor's flow fields. To prevent the onset of these instabilities or, at least, minimize their detrimental effects (e.g., through active control), an understanding of the processes that control these instabilities is needed. This requires an understanding of the processes that: (1) amplify (i.e., destabilize) inherent disturbances in the system, (2) control the transient behavior of the disturbances in the combustor (e.g., during active control, or as the combustor transitions from stable to unstable operation), and (3) cause the amplitude of the unsteady motions to saturate into a limit cycle.

Although far from complete, current understanding of these processes in premixed combustors has significantly improved as a result of extensive experimental (e.g., Refs. [1–4]) and theoretical (e.g., Refs. [4–6]) investigations. For example, there is reasonable agreement between experimental [2,3] and theoretical [4] studies of the key parameters that control their stability characteristics, suggesting that the dominant linear processes responsible for initiating these instabilities are understood. Furthermore, significant improvements in understanding of the non-linear behavior of these systems through perturbation and dynamical systems analyses have provided a rational framework for characterizing their inherently non-linear oscillatory behavior (e.g., stability boundary hysteresis, mode selection, limit cycles) [6–11].

While many of the linear and non-linear features of these oscillations have been analyzed and interpreted within a deterministic framework, their stochastic characteristics have received considerably less attention. Yet, extensive analysis of measured data [4] suggests that these oscillations have random features that cannot be characterized within an entirely deterministic framework. For example, the amplitude and phase of the limit cycle oscillations vary from cycle to cycle in a seemingly random manner. Also, the parameter values defining the combustor stability boundaries vary somewhat from test to test (e.g., on the order of five percent in our combustor). Such variability may be significant in modern high-performance combustion systems that must often operate near stability boundaries in order to minimize pollutant emissions [1].

These stochastic characteristics are likely due to the fact that combustion instabilities occur in a very "noisy", turbulent flow environment that can, in some cases, cause qualitative changes in the combustor's dynamics. Theoretical analyses by Culick et al. [8], Burnley [12] and Clavin et al. [13] have suggested that, because of the presence of this background noise, the instability characteristics (e.g., the instability amplitude) are random variables. Thus, it is more appropriate to characterize the instability characteristics by their statistical characteristics (e.g., their probability density function) than by a single deterministic quantity.

These theoretical analyses and experimental observations of apparently stochastic features in measured data [4] suggested that additional insight into the characteristics of combustion instabilities could be obtained by statistical analysis of these features. As such, we performed an analysis of the statistical characteristics of the cycle-to-cycle variability of the amplitude and phase of the combustor pressure that is described below. Specifically, the next section presents typical combustor pressure data and analyzes the probability density functions (PDFs) of the pressure amplitude and phase. These results are then compared with the statistical characteristics of the amplitude and phase of a randomly forced, non-linear oscillator equation that is similar to those investigated in other combustion instability studies [8,10,11]. Solutions of this model are presented and shown to be in good agreement with the measured data.

2. Statistical characteristics of measured pressure data

This section presents typical data illustrating the statistical characteristics of the unsteady pressure amplitude and phase. These data were obtained from a lean, premixed gas turbine combustor simulator that is described in detail in Ref. [4]. They were measured with a Model 211B5 Kistler pressure transducer that was sampled at 2000 Hz. A typical time series of the combustor pressure and its Fourier transform during a 204 Hz instability are shown in Figs. 1 and 2, respectively. These figures show that the pressure oscillates periodically with a frequency content that is dominated by the 204 Hz mode. Although these pressure oscillations exhibit significant temporal coherence (as shown by their autocorrelations, see Ref. [4]), they also vary somewhat from cycle to cycle. These cyclic variations are apparent in the state space evolution of the pressure, which allows for a comparison of the pressure oscillations over several hundred cycles. Fig. 3 plots the time dependence of the vector $[p'(t)\Delta p'(t)/\Delta t]$ over 100 cycles of oscillation, where $\Delta p'(t) = p'(t + \Delta t) - p'(t)$ and Δt is the inverse of the sampling frequency. Fig. 3 shows that the pressure is executing an "average" orbit that differs slightly from one cycle to the next. Although we do not present it here, an extensive investigation of this variability has shown that it is uncorrelated from one cycle to the next, suggesting that it is caused by high degree of freedom processes with short correlation times relative to the acoustic period [4,14].

Our failure to determine a low-dimensional deterministic source to this variability motivated an analysis of its statistical characteristics. This data analysis was performed using the following

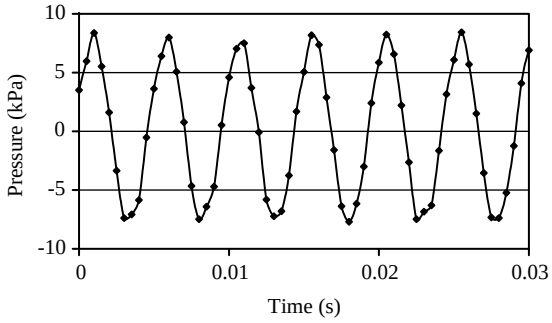

Fig. 1. Typical time series of the combustor pressure during a 204 Hz instability ($\bar{\phi} = 0.85$, $\overline{\dot{m}} = 16$ g/s, $\bar{p} = 6.68$ atm).

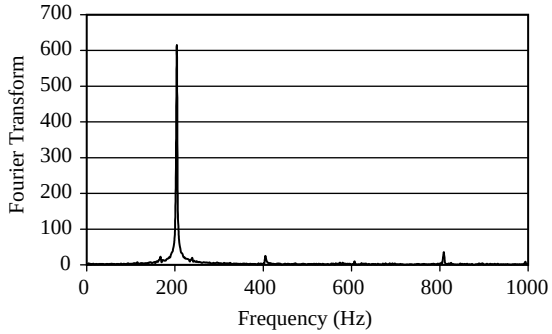

Fig. 2. Fourier transform of the combustor pressure for the operating conditions shown in Fig. 1.

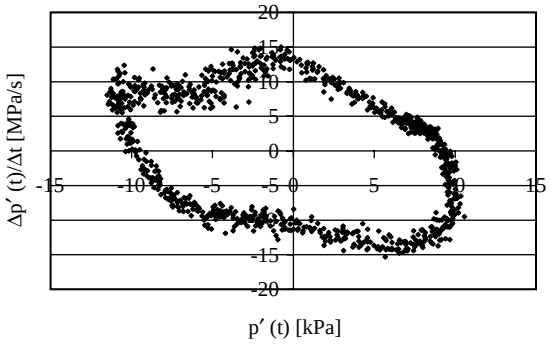

Fig. 3. Phase portrait of the combustor pressure for the operating conditions shown in Fig. 1.

procedure: (1) determine a "reference" signal, $S(t) = \cos(\omega t + \sigma)$, whose angular frequency, ω, was determined from the average value of the frequency of the pressure oscillations, and phase, σ, was chosen to equal that of the data for the first cycle of oscillation, (2) divide the data record and reference signal into N ensembles, (3) determine the pressure amplitude, A_n, and phase (with respect to reference signal), σ_n, using the Hamming windowed, Fourier transform of the time series data in each ensemble (where $n = 1, 2, \ldots, N$), and (4) determine the PDFs of the pressure Fourier transform amplitude and phase (at the frequency of the reference signal) based upon the N values of A_n and σ_n.

This procedure is most easily applied to a time series composed of harmonic oscillations; i.e., to pressure data obtained during an instability. However, during stable operation the pressure oscillates in a somewhat random fashion. Reference to its Fourier transform under these conditions reveals a broadband background, with small peaks at the natural acoustic frequencies of the combustor. When analyzing stable combustor pressure data, we determined the amplitude of the oscillations of these natural acoustic modes in the same manner as described above. We did not, however, determine any phase information during stable operation because defining a "reference" signal is ambiguous in this situation. It should also be noted that while the above procedure was outlined for a signal composed of only one harmonic component, it can be readily generalized to a multi-mode time series as well.

We now present data illustrating the typical statistical characteristics of the 204 Hz mode of the combustor pressure. These data were obtained from time series records of 131,072 data points that were divided into $N = 2048$ ensembles (the choice of N is somewhat arbitrary; e.g., we found that doubling or halving it produced similar results). Typical PDFs of the pressure amplitude obtained under three different *stable* operating conditions[1] are shown in Fig. 4. These operating conditions range from "very stable" (far left curve) to near the stability limit (far right curve). These operating conditions were changed by varying the degree of constriction of a back pressure

[1] Determining whether a combustor is "stable" or "unstable" at a particular operating condition is not a trivial question. Our determination of stability is based upon autocorrelation analysis of the data, as described in Ref. [4]. See also discussion in the next paragraph of the text.

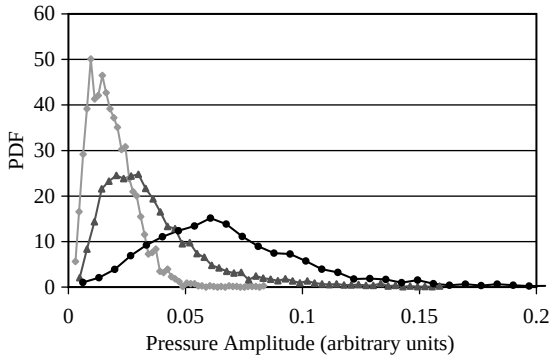

Fig. 4. Typical probability density functions of the 204 Hz mode pressure amplitude during stable operation ($\bar{\phi} = 0.85$, $\bar{\dot{m}} = 16$ g/s); ♦, $\bar{p} = 6.58$ atm; ▲, 6.60 atm; ■, 6.71 atm.

valve on the combustor exhaust that, in turn, controlled the mean combustor pressure.[2] Examination of Fig. 4 shows that the far left PDF ($\bar{p} = 6.58$ atm) corresponding to the "most stable" operating conditions peaks at a low amplitude and remains in a narrow range of values. This PDF is also asymmetric with a tail that extends toward the higher amplitude values and resembles a Rayleigh distribution. The PDF of the middle curve ($\bar{p} = 6.60$ atm), corresponding to operating conditions that are closer to the combustor's stability limit, peaks at a slightly larger amplitude. Note that while these two PDFs peak at different amplitudes, they are qualitatively similar in shape. However, the $\bar{p} = 6.60$ atm PDF is significantly broader than the lower amplitude PDF, implying that the oscillations exhibit a wider range of amplitudes as the combustor moves closer to the stability limit.

Next, consider the PDF obtained at a mean pressure of $\bar{p} = 6.71$ atm whose PDF peaks at the largest pressure amplitude. These data were obtained very near the combustor's stability boundary. In fact, further changes in operating conditions resulted in the combustor becoming unstable (as evidenced by a sudden jump in amplitude of the pressure oscillations, see also Ref. [4]). Examination of this PDF reveals that the oscillatory amplitude spans an even broader range of values than in the two previously discussed, lower amplitude cases. Furthermore, in contrast to the other two PDFs, it is nearly symmetric about its peak value. Thus, these data show that the amplitude PDFs become monotonically broader and transition from an asymmetric to a symmetric distribution as the combustor approaches the stability limit.

We next compare these PDFs with those obtained under *unstable* operating conditions, see Fig. 5. These data were obtained by varying the operating conditions in the same manner as discussed above. Note that there is some overlap in the values of the mean pressures of these data with those shown in Fig. 4. This overlap reflects the hysteresis in stability boundaries that has been also noted by other investigators [3,4].

Fig. 5 shows that the shapes of all three PDFs are quite similar, although their mean amplitudes are different. Specifically, these PDFs are all symmetric and resemble Gaussian-type distributions.

[2] Because the reactants mass flow rates were kept constant, changes in the mean combustor pressure caused a change in the combustor inlet velocity [4]. Such changes in inlet velocity in our combustor strongly influence its stability characteristics, likely because they affect the convective time between the fuel injection point and the flame, see Ref. [4].

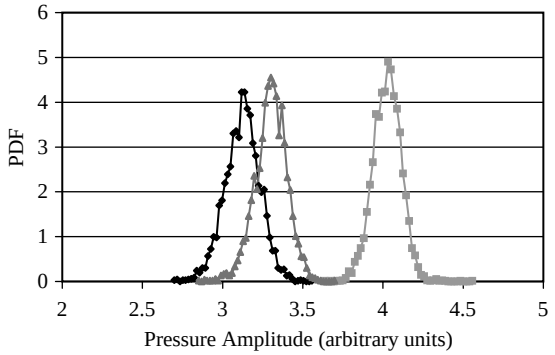

Fig. 5. Typical probability density functions of the 204 Hz mode pressure amplitude during unstable operation ($\bar{\phi} = 0.85$, $\overline{\dot{m}} = 16$ g/s); ♦, $\bar{p} = 6.65$ atm; ▲, 6.68 atm; ■, 6.71 atm.

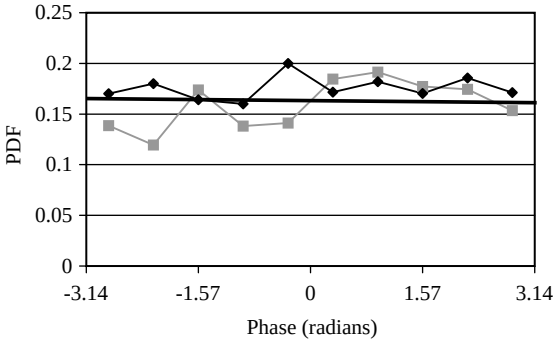

Fig. 6. Comparison of the experimental probability density functions of the 204 Hz mode of the phase of the combustor pressure during an instability ($\bar{\phi} = 0.85$, $\overline{\dot{m}} = 16$ g/s) with Eq. (16); ♦, $\bar{p} = 6.68$ atm; ■, 6.71 atm; —, predicted PDF, Eq. (16).

The only significant difference between the three curves is the narrowing width of the PDFs with increasing amplitude (since the area under each curve is the same, this decreasing width can be noted by comparing the peak height of the PDFs). Thus, these data show that the instability amplitude takes a smaller and smaller range of values as its magnitude increases.

Fig. 6 presents typical PDFs of the phase of the oscillations during unstable operation (recall that no phase information was determined during stable operation). The figure shows that the instability phase is nearly uniformly distributed between $-\pi$ through π radians with respect to the reference signal. This result shows that the phase of the pressure oscillations drifts and, given enough cycles, takes all values with a nearly uniform probability. Further analysis of this phase drift is presented in Ref. [14], showing that it resembles features exhibited by random walk models, similar to those used to describe other random processes (such as Brownian motion).

These data in Figs. 4–6 illustrate the principle statistical characteristics of the pressure amplitude and phase. The next section compares these data with the statistical characteristics of a non-linear oscillator forced by random noise.

3. Theoretical analysis

The analysis in this section is based upon prior studies of Zinn and coworkers [11] and Culick and coworkers [8,10] who have shown that acoustic oscillations in combustion chambers can be modelled as the superposition of non-linearly interacting oscillators, where each oscillator typically represents a natural acoustic mode of the combustor. Accordingly, by retaining the contributions of the first m modes of oscillation, the pressure at a single point in the combustor can be written as

$$p'(t) = \sum_{i=1}^{m} \eta_i(t), \tag{1}$$

$$\frac{\mathrm{d}^2\eta_i(t)}{\mathrm{d}t^2} + \omega_i^2\eta_i(t) = \frac{\alpha_i}{\omega_i}\frac{\mathrm{d}\eta_i(t)}{\mathrm{d}t} + \theta_i\eta_i(t) - \hat{f}\left(\eta_j(t), \frac{\mathrm{d}\eta_j(t)}{\mathrm{d}t}, \ldots\right), \quad i, j = 1, 2, \ldots, m, \tag{2}$$

where the function $\hat{f}$ describes the non-linearities in the system (specific expressions for $\hat{f}$ that are introduced by gas dynamical or combustion processes are derived in Refs. [10,11]). Consider the following modified form of Eq. (2) that incorporates the effects of temporal perturbations of the system parameters and external forcing of the oscillators by "background noise" (e.g., by turbulent fluctuations) in the combustor:

$$\frac{\mathrm{d}^2\eta_i(t)}{\mathrm{d}t^2} + \omega_i^2\eta_i(t) = \left(\frac{\alpha_i + \tilde{\alpha}_i(t)}{\omega_i}\right)\frac{\mathrm{d}\eta_i(t)}{\mathrm{d}t} + (\theta_i + \tilde{\theta}_i(t))\eta_i(t) - \left((\hat{f}+\tilde{f})\left(\eta_j(t), \frac{\mathrm{d}\eta_j(t)}{\mathrm{d}t}, \ldots\right)\right) + \xi_i(t),$$
$$i, j = 1, 2, \ldots m, \tag{3}$$

where $\tilde{\alpha}_i(t)$, $\tilde{\theta}_i(t)$, and $\tilde{f}$ denote parametric disturbances of the instability growth rate, frequency, and system non-linearities, respectively, and $\xi_i(t)$ denotes an external excitation. A similar equation was previously considered in the context of combustion instabilities by Culick et al. [8] in an analysis of two combustor modes that were coupled through non-linear gas dynamical processes.

To reduce the complexity of this system of equations while retaining the important physical features of the investigated problem we assume that: (1) the unsteady pressure is dominated by the oscillations of a single mode that interacts non-linearly with itself, (2) the parametric excitation terms are negligible relative to the additive noise term, (3) the correlation time of the external excitation is small relative to the other pertinent time scales of the problem and, thus, $\xi(t)$ is idealized as a random, white noise source, and (4) the terms on the right-hand side of Eq. (3) are "small" (more precise treatments on what it means for these quantities to be "small" are given in Refs. [8,15]).

Assumption (1) is based upon the results of several experimental and theoretical investigations of non-linear oscillations in lean, premixed gas turbine combustors [4,6,9].[3] Assumption (2) is based upon prior analysis [15] showing that the dominant characteristics of the pressure PDF are

[3] It should be noted, however, that this assumption would be inappropriate for analyses of large amplitude instabilities in other combustion systems, such as rockets or ramjets, where it is known that gas dynamical coupling between multiple combustor modes plays a key role in the combustor's dynamics [8,10,11]. In these cases, the analysis of Culick et al. [8] or the Monte-Carlo simulations of Burnley [12] are more appropriate.

captured with a model that only retains additive noise terms (it should be emphasized, as noted in Ref. [15], that these neglected parametric noise terms can introduce changes in the combustor stability boundary and increased probability of large excursions of the pressure amplitude). Assumption (3) is based upon autocorrelation analysis of these pressure data (see Ref. [4]). Finally, assumption (4) is based upon numerous experimental and theoretical results showing that the limit cycle oscillations in these combustors can, in many cases, be described by a weakly non-linear theory [4,6,10,11].

With these assumptions, Eqs. (1) and (3) are combined to yield

$$\frac{\mathrm{d}^2p'(t)}{\mathrm{d}t^2}+\omega^2p'(t)=\frac{\alpha}{\omega}\frac{\mathrm{d}p'(t)}{\mathrm{d}t}+\theta p'(t)-\hat{f}\left(p'(t),\frac{\mathrm{d}p'(t)}{\mathrm{d}t}\right)+\xi(t)$$
$$=-f\left(p'(t),\frac{\mathrm{d}p'(t)}{\mathrm{d}t}\right)+\xi(t). \tag{4}$$

Eq. (4) is the resulting model non-linear oscillator equation considered in this study. The objective of the ensuing analysis is to study its statistical characteristics and compare them with the data in the prior section. The statistical characteristics of this equation has been analyzed extensively, and so we do not present extensive details of the solution procedure. Such details can be found in other analyses [8,16–18].

Since the pressure oscillations are nearly harmonic, it is convenient to decompose $p'(t)$ and $\mathrm{d}p'(t)/\mathrm{d}t$ as [8,16]

$$p'(t)=A(t)\cos(\omega t+\sigma(t)), \tag{5}$$

$$\mathrm{d}p'(t)/\mathrm{d}t=-A(t)\omega\sin\omega(t+\sigma(t)), \tag{6}$$

where $A(t)$ and $\sigma(t)$ denote the fluctuating amplitude and phase of the oscillations. Using Eqs. (5) and (6), Eq. (4) can be rewritten as the following set of first order differential equations for the instability amplitude and phase [16]:

$$\frac{\mathrm{d}A(t)}{\mathrm{d}t}=\frac{\sin\Phi}{\omega}(f(A\cos\Phi,-A\,\omega\sin\Phi)-\xi(t)), \tag{7}$$

$$\frac{\mathrm{d}\sigma(t)}{\mathrm{d}t}=\frac{\cos\Phi}{A\omega}(f(A\cos\Phi,-A\,\omega\sin\Phi)-\xi(t)), \tag{8}$$

where $\Phi=\omega t+\sigma(t)$. Assuming that amplitude and phase changes occur over time scales that are long relative to the acoustic period, these equations can be considerably simplified by time averaging, see Refs. [8,16,18]. The resulting time averaged, stochastic Ito equations for the instability amplitude and phase are given by [16]

$$\mathrm{d}A=\left(-\frac{F(A)}{\omega}+\frac{\pi S(\omega,\,t)}{2A\omega^2}\right)\mathrm{d}t-\frac{\sqrt{\pi S(\omega,\,t)}}{\omega}\mathrm{d}\,Y_1(t), \tag{9}$$

$$\mathrm{d}\sigma=-\frac{G(A)}{A\omega}\mathrm{d}t-\frac{\sqrt{\pi S(\omega,\,t)}}{A\omega}\mathrm{d}\,Y_2(t), \tag{10}$$

where $Y_1(t)$ and $Y_2(t)$ are two independent, unit Wiener processes, $S(\omega, t)$ is the power spectral density of the random excitation at time, t, and angular frequency, ω, and

$$F(A) = -\frac{1}{2\pi}\int_0^{2\pi} f(A\cos\Phi, -A\,\omega\sin\Phi)\sin\Phi\,\mathrm{d}\Phi, \tag{11}$$

$$G(A) = -\frac{1}{2\pi}\int_0^{2\pi} f(A\cos\Phi, -A\,\omega\sin\Phi)\cos\Phi\,\mathrm{d}\Phi, \tag{12}$$

The temporal evolution of the *statistical* characteristics of $A(t)$ and $\sigma(t)$ are described by the transition density function, $P(A, \sigma, t|A_1, \sigma_1, t_1)$, which is obtained from the Fokker–Planck Eq. [16]. Examination of Eq. (9) shows that the amplitude is decoupled from the phase, implying that $A(t)$ is a one-dimensional Markov process. It can be shown that its transition density function, $P_A(t) = P(A, t|A, t_1)$, is given by the following Fokker–Planck equation [16]:

$$\frac{\partial P_A}{\partial t} = \frac{\partial}{\partial A}\left[\left(\frac{F(A)}{\omega} - \frac{\pi S(\omega, t)}{2A\omega^2}\right)P_A\right] + \frac{\pi S(\omega, t)}{2\omega^2}\frac{\partial^2 P_A}{\partial A^2}. \tag{13}$$

Similarly, the Fokker–Planck equation of the joint Markov process (A, σ), described by Eq. (10), is given by

$$\frac{\partial P_\sigma}{\partial t} = \frac{\partial}{\partial A}\left[\left(\frac{F(A)}{\omega} - \frac{\pi S(\omega, t)}{2A\omega^2}\right)P_\sigma\right] + \frac{G(A)}{A\omega}\frac{\partial P_\sigma}{\partial \sigma} + \frac{\pi S(\omega, t)}{2\omega^2}\left[\frac{\partial^2 P_\sigma}{\partial A^2} + \frac{1}{A^2}\frac{\partial^2 P_\sigma}{\partial \sigma^2}\right], \tag{14}$$

where $P_\sigma(t) = P(A, \sigma, t|A_1, \sigma_1, t_1)$. No general solutions of Eqs. (13) and (14) are known except in cases where P_σ and P_A are stationary (i.e., independent of time). For the stationary case, the solutions for the PDFs of A and σ, $W(A)$ and $W(\sigma)$, are

$$W(A) = CA\mathrm{e}^{-(2\omega/(\pi S(\omega)))\int_0^A F(\psi)\,\mathrm{d}\psi}, \tag{15}$$

$$W(\sigma) = 1/2\pi, \tag{16}$$

where C is a normalizing constant.

Note that no additional assumptions about the function f, other than the above assumption (4), were made to obtain Eqs. (15) and (16). Eqs. (11) and (15) show that the amplitude PDF, $W(A)$, depends upon the system non-linearities and instability growth rate through the function $F(A)$. Significantly, Eq. (16) shows that the phase PDF, $W(\sigma)$, is uniform; i.e., there is equal probability that $\sigma(t)$ will equal any value, $-\pi < \sigma < \pi$. This result is true regardless of the system parameters and nonlinearities.

In order to complete the analytical description of $W(A)$ in Eq. (15), it is necessary to derive an expression for the function F(A). This can be accomplished in a general fashion by expanding the

function $f(p', \mathrm{d}p'/\mathrm{d}t)$ (see Eq. (4)) in the following Taylor series:

$$f(p', \mathrm{d}p'/\mathrm{d}t) = -\theta p' - \frac{\alpha}{\omega}\frac{\mathrm{d}p'}{\mathrm{d}t} + b_{20}p'^2 + \frac{b_{02}}{\omega^2}\left(\frac{\mathrm{d}p'}{\mathrm{d}t}\right)^2 + \frac{b_{11}}{\omega}p'\frac{\mathrm{d}p'}{\mathrm{d}t} + b_{30}p'^3 + \frac{b_{21}}{\omega}p'^2\frac{\mathrm{d}p'}{\mathrm{d}t} + \frac{b_{12}}{\omega^2}p'\left(\frac{\mathrm{d}p'}{\mathrm{d}t}\right)^2 + \frac{b_{03}}{\omega^3}\left(\frac{\mathrm{d}p'}{\mathrm{d}t}\right)^3 + b_{40}p'^4 + \frac{b_{31}}{\omega}p'^3\frac{\mathrm{d}p'}{\mathrm{d}t} + \frac{b_{22}}{\omega^2}p'^2\left(\frac{\mathrm{d}p'}{\mathrm{d}t}\right)^2 + \frac{b_{13}}{\omega^3}p'\left(\frac{\mathrm{d}p'}{\mathrm{d}t}\right)^3 + \frac{b_{04}}{\omega^4}\left(\frac{\mathrm{d}p'}{\mathrm{d}t}\right)^4, \tag{17}$$

where the b_{ij}'s are constants. Although $f(p', \mathrm{d}p'/\mathrm{d}t)$ is truncated at fourth order in Eq. (17), it can be expanded to an arbitrary order in a straightforward manner. Substituting Eq. (17) into Eq. (11) yields

$$F(A) = -\frac{\alpha A}{2} + \left(\frac{3b_{03} + b_{21}}{8}\right)A^3 + \cdots = -\frac{\alpha A}{2} + k^2A^3 + \cdots, \tag{18}$$

where $k^2 = (3b_{03} + b_{21})/8$.[4] Eq. (18) shows that only three out of the 14 terms in Eq. (17) contribute to $F(A)$. Furthermore, two out of the three non-linearities combine into a single cubic term. Inserting Eq. (18) into Eq. (15) yields the final result for the PDF of the mode's amplitude,

$$W(A) = \frac{\sqrt{8k^2\omega/(\pi^2 S(\omega))}\,\mathrm{e}^{-\alpha^2\omega/(8\pi k^2 S(\omega))}}{1 + \mathrm{erf}\sqrt{\alpha^2\omega/(8\pi k^2 S(\omega))}} A\mathrm{e}^{\omega A^2(\alpha - k^2A^2)/(2\pi S(\omega))}. \tag{19}$$

Eq. (19) shows that the amplitude PDF depends upon the combustors linear and non-linear characteristics through the parameters α and k^2, and the background noise characteristics through the power spectral density of the noise, $S(\omega)$. Although $W(A)$ exhibits a quantitative dependence upon five parameters, we will next show that its qualitative characteristics can be reduced to its dependence upon a single parameter. This is accomplished by introducing the dimensionless amplitude $\tilde{A} = \sqrt[4]{\omega k^2/(2\pi S(\omega))}A$ and substituting it into Eq. (19):

$$W(\tilde{A}) = \frac{4}{\sqrt{\pi}}\frac{\mathrm{e}^{-\Omega^2/4}}{1 + \mathrm{erf}(\Omega/2)}\tilde{A}\mathrm{e}^{\tilde{A}^2(\Omega - \tilde{A}^2)}, \tag{20}$$

where

$$\Omega = \frac{\alpha}{|k|}\sqrt{\frac{\omega}{2\pi S(\omega)}}. \tag{21}$$

Equation (20) shows that the normalized amplitude PDF, $W(\tilde{A})$, depends upon the single parameter, Ω. Note that Ω is negative and positive when the combustor is linearly stable ($\alpha < 0$) and unstable ($\alpha > 0$), respectively, see Eq. (21). Figs. 7 and 8 plot the dependence of $W(\tilde{A})$ upon $\tilde{A}$ for several values of Ω that correspond to stable and unstable operating conditions, respectively (thus, describing the variations of the amplitude PDF as the combustor transitions from stable to unstable operation).

[4] Since the coefficient $(3b_{03} + b_{21})/8$ that multiplies the A^3 term in Eq. (18) must be positive in order for $W(A)$ to have physical meaning, we express this coefficient as k^2. If this coefficient is not positive, then truncating the Taylor series expansion of $f(p', \mathrm{d}p'/\mathrm{d}t)$ to fourth order as done in Eq. (17) is inappropriate and higher order terms must be retained.

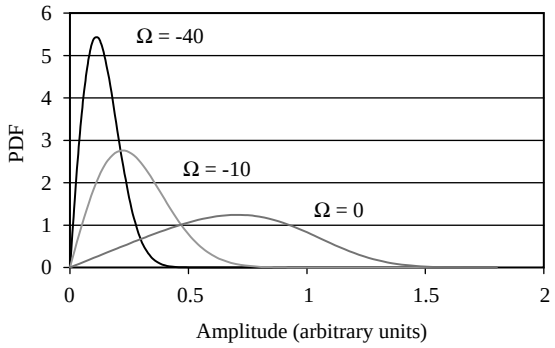

Fig. 7. Predicted dependence of the amplitude probability density function (obtained from Eq. (20)) of a stable combustor mode excited by random noise.

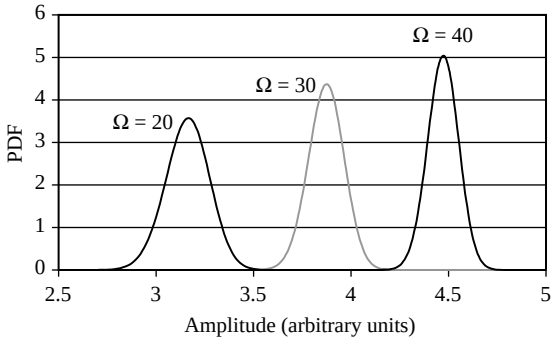

Fig. 8. Predicted dependence of the amplitude probability density function (obtained from Eq. (20)) of an unstable combustor mode excited by random noise.

Comparison of the results in Figs. 7 and 8 with the measurements in Figs. 4 and 5 shows a good agreement between the predicted and measured amplitude PDFs. Specifically, the experimental and predicted PDFs exhibit similar transitions from asymmetric to symmetric profiles as the combustor moves from stable to unstable operation. They also show the transition from a narrowly distributed PDF under stable conditions, the broadening of the PDF as the stability limit is approached, and the narrowing of the PDF with increasing instability amplitude.

Since the actual values of the parameter Ω for the experimental data are unknown, the above amplitude PDF comparisons are only qualitative. Quantitative comparisons between the predicted and measured phase PDFs are possible, however, because of the simplicity of the predicted PDF of $W(\sigma)$, see Fig. 6. Fig. 6 shows that the measured and predicted (see Eq. (16)) phase PDFs are also in good agreement. This good agreement between the measured and predicted statistical characteristics of the instability amplitude and phase suggests that the studied model equation (4) captures many of the random features of the cycle-to-cycle variations of the pressure oscillations. This qualitative agreement also supports the conjectures of several prior studies [4,6,9], which suggested that unstable gas turbine combustor dynamics can be described by a single oscillator that interacts non-linearly with itself.

In closing, we briefly summarize the effects of background noise upon the characteristics of self-excited, combustion-driven oscillations. First, as shown explicitly above, background noise causes the instability phase to drift and, given enough cycles, to achieve uniform probability of having all values. A second effect that is predicted by the model is a reduction in the mean instability amplitude. Such a change in the mean characteristics of non-linear systems by background noise is well known [19], and in this case is due to non-linear interactions between the coherent, self-excited oscillations and the random oscillations. The predicted dependence of the mean instability amplitude, normalized by its value in the absence of noise, upon the noise levels is plotted in Fig. 9. The mean amplitude was calculated using the expression

$$\langle A \rangle = \int_0^\infty A W(A)\, \mathrm{d}A, \tag{22}$$

where $W(A)$ is given by Eq. (19). As shown in the figure, the instability amplitude decreases slightly as the parameter $4\pi k^2 S(\omega)/\omega\alpha^2$ increases, but the effect is not large and amounts to a reduction of only a few percent. Although not shown here, the predicted mean amplitude actually begins to increase for larger background noise levels. We do not show these results because the perturbation theory used in this analysis is valid for small noise levels, and may not be valid at

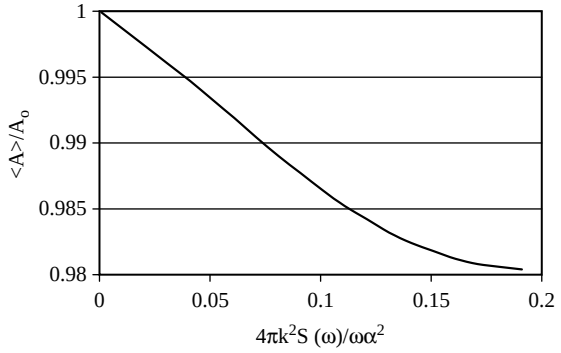

Fig. 9. Predicted dependence (from Eqs. (20) and (22)) of mean instability amplitude, $\langle A \rangle$, normalized by its value in the absence of background noise, A_o, upon the parameter $4\pi k^2 S(\omega)/\omega\alpha^2$.

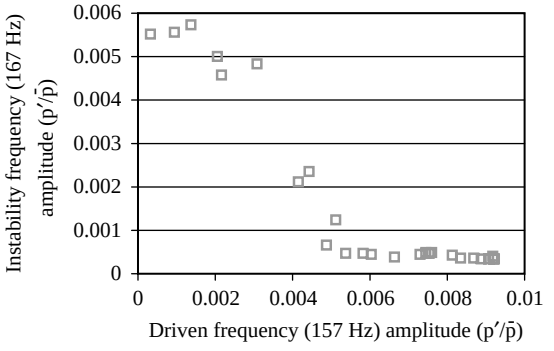

Fig. 10. Dependence of instability frequency amplitude upon the driven frequency amplitude (data obtained from Ref. [20]).

these higher levels. Nonetheless, they do suggest that background noise may have very significant effects upon the instability characteristics for larger values of $4\pi k^2 S(\omega)/\omega\alpha^2$, such as when the combustor is only weakly unstable; i.e., $\alpha \sim 0$.

Because of the difficulty in imposing different background noise levels upon the system during tests, we do not have direct experimental verification of this dependence of instability amplitude upon background noise levels. However, we have obtained related data in tests where coherent oscillations were externally driven at frequencies close to the instability frequency [20], see Fig. 10. These tests were performed for a different combustor configuration where the instability frequency was 167 Hz. Harmonic oscillations of varying amplitude were driven at a frequency of 157 Hz. In such a case, non-linear oscillations theory predicts that the amplitude of the self-excited oscillations decreases with increasing amplitude of driven oscillations; this phenomenon is known as entrainment or frequency locking [18]. As shown in the figure, the instability amplitude progressively decreases with increasing drive amplitude, in agreement with the theory in Ref. [18]. Although this phenomenon is not directly related to the studied phenomenon of noise effects upon instability amplitude, they have similarities in their demonstration that non-linear interactions between self-excited oscillations and driven oscillations affect the instability characteristics.

4. Final comments

The results of this paper have several implications on current understanding and active control of combustion instabilities. First, they emphasize the inherently stochastic features of combustor pressure oscillations. Although the presence of such stochastic characteristics implies that there will always exist some lack of repeatability from one cycle or test to the next, it also shows that a statistical characterization of such variability may yield further insight into the characteristics of the system. For example, the agreement between the model and data lends indirect support to prior conjectures that unstable gas turbine combustor dynamics can be described by a single oscillator that interacts non-linearly with itself [4,6,9].

Next, the good agreement between the measured and predicted statistical characteristics of the instability amplitude and phase suggests that the studied model equation (4) captures many of the random features of the cycle-to-cycle variations of the pressure oscillations. This agreement suggests that the analysis presented in this paper provides a useful framework for interpreting other random features of combustor stability characteristics; e.g., cyclic variability (addressed in this paper), "fuzziness" in stability boundaries, or noise induced transitions [4].

Finally, these results serve as reminders that active control systems (ACS) must account for the inherent noise in the system and its affect upon the oscillations. For example, the data in Fig. 6 implies that the instability phase continuously drifts (on the order of a degree every two cycles [14]). Thus, in order for the ACS to be effective, the time scales associated with its observation, analysis, and actuation must be small relative to the time scales of the phase drift.

Acknowledgements

This research was partially supported by AGTSR under Contract No. 95-01-SR031.

Appendix A. Nomenclature

A	amplitude of oscillation
b	Taylor series coefficients, see Eq. (17)
f	oscillator forcing function, see Eq. (4)
F	time-averaged oscillator forcing function, see Eq. (11)
$\dot{m}$	mass flow rate
N	number of ensembles data record is divided into
p'	unsteady pressure
$\bar{p}$	mean pressure
S	power spectral density
W	probability density function
Y	Wiener process

Greek letters

α	instability growth rate, see Eq. (2)
ϕ	equivalence ratio
θ	frequency shift, see Eq. (2)
σ	phase of oscillations
ω	angular frequency
Ω	amplitude PDF parameter, see Eq. (21)

References

[1] J. Cohen, T. Anderson, Experimental investigation of near-blowout instabilities in a lean premixed combustor, AIAA paper # 96-0819, 1996.
[2] J.C. Broda, S. Seo, R.J. Santoro, G. Shirhattikar, V. Yang, An experimental study of combustion dynamics of a premixed swirl injector, Proceedings of the Combustion Institute 27 (1998).
[3] D.L. Straub, G.A. Richards, Effect of fuel nozzle configuration on premix combustion dynamics, ASME paper # 98-GT-492, 1998.
[4] T. Lieuwen, Experimental investigation of limit cycle oscillations in an unstable gas turbine combustor, Journal of Propulsion and Power 18 (1) (2002) 61–67.
[5] T. Lieuwen, B.T. Zinn, The role of equivalence ratio oscillations in driving combustion instabilities in low NO_x gas turbines, Proceedings of the Combustion Institute 27 (1998).
[6] A.A. Peracchio, W.M. Proscia, Nonlinear heat release/acoustic model for thermo-acoustic instability in lean premixed combustors, ASME paper # 98-GT-269, 1998.
[7] C.A. Jacobsen, A.I. Khibnik, A. Banaszuk, J. Cohen, W. Proscia, Active control of combustion instabilities in gas turbine engines for low emissions. Part I: physics based and experimentally identified models of combustion instability, AVI 2000.
[8] F.E.C. Culick, L. Paparizos, J. Sterling, V. Burnley, Combustion noise and combustion instabilities in propulsion systems, Proceedings of the AGARD Conference on Combat Aircraft Noise, AGARD CP 512, 1992.
[9] A. Dowling, Nonlinear self excited oscillations of a ducted flame, Journal of Fluid Mechanics 346 (1997) 271–290.
[10] F.E.C. Culick, V. Burnley, G. Swenson, Pulsed instabilities in solid-propellant rockets, Journal of Propulsion and Power 11 (4) (1995) 657–665.

[11] B.T. Zinn, E.A. Powell, Nonlinear combustion instability in liquid propellant rocket engines, Proceedings of the Combustion Institute 13 (1970).
[12] V. Burnley, Nonlinear Combustion Instabilities and Stochastic Sources, Ph.D.Thesis, California Institute of Technology, 1996.
[13] P. Clavin, J.S. Kim, F.A. Williams, Turbulence induced noise effects on high frequency combustion instabilities, Combustion Science Technology 96 (1994) 61–84.
[14] T. Lieuwen, Phase drift characteristics of self excited, combustion driven oscillations, Journal of Sound and Vibration 242 (5) (2001) 893–905.
[15] T. Lieuwen, A. Banaszuk, Background noise effects on combustor stability, ASME paper # 2002-GT-30062, 2002.
[16] J.B. Roberts, J.D. Spanos, Stochastic averaging: an approximate method of solving random vibration problems, International Journal of Nonlinear Mechanics 21 (2) (1986) 111–134.
[17] A. Preumont, Random Vibration and Spectral Analysis, Kluwer Academic Publishers, Dordrecht, 1994.
[18] A. Nayfeh, D. Mook, Nonlinear Oscillations, Wiley, New York, 1995.
[19] W. Horsthemke, R. Lefever, Noise Induced Transitions: Theory and Applications in Physics, Chemistry, and Biology, Springer, Berlin, 1984.
[20] T. Lieuwen, Y. Neumeier, Nonlinear pressure-heat release transfer function measurements in a premixed combustor, Proceedings of the Combustion Institute 29 (2002).